HAIT Journal of Science and Engineering, Volume 1, Issue 3, pp. 470-497

Non-uniform two-dimensional electron gas in a magnetic field

Alexander Shik

Centre for Advanced Nanotechnology,
University of Toronto, Toronto M5S 3E4, Canada
e-mail: shik@ecf.utoronto.ca
Received 8 September 2004, accepted 13 October 2004

Abstract

Basic properties of a two-dimensional electron gas with spatially varying carrier concentration in external magnetic fields are reviewed. The two main problems: modification of galvanomagnetic coefficients due to random fluctuations of equilibrium concentration and the concentration gradient created by the Lorenz force in the Hall direction – are considered for weak, classically strong, and quantizing magnetic fields. The screening of concentration non-uniformities under the quantum Hall conditions are discussed separately.

PACS: 75.47.-m, 71.70.Di

1 Introduction

This paper represents a review devoted to the influence of sample inhomogeneity on a wide class of transport phenomena in a two-dimensional (2D) electron gas in a low, high and quantized magnetic field **H** perpendicular to its plane. Such inhomogeneities are a privilege of a very wide class of semiconducting materials including strongly compensated, irradiated, polycrystalline, amorphous and some other [1]. All of them can be described by a general model of a semiconductor with energy band modulated by some random potential $V(x, y)$ (we assume the 2D gas to occupy the plane $z = 0$). Such an approach will be used here as well.

2 Classical magnetic field

2.1 Conductivity and Hall effect of non-uniform samples

This subsection is devoted to the standard transport problem of non-uniform samples, which can be formulated in the following way. Let us have a 2D sample with a spatially varying conductivity $\sigma(x, y)$ provided with macroscopic contacts having the size considerably larger that the characteristic size of inhomogeneities L. In this case, the measured values of effective diagonal σ_{xx} and non-diagonal (Hall) σ_{xy} conductivity, determined as a ratio of average corresponding components of electric field and current density, are independent of the size and position of contacts and determined only by some statistical characteristics of $\sigma(x, y)$ [1].

To solve this problem exactly, we must find spatial distributions of the in-plane (2D) electric field $\mathbf{E}(x, y)$ and current density $\mathbf{j}$ (x, y) by solving the equation system

$$\operatorname{div} \mathbf{j}(x, y) = 0, \qquad \operatorname{curl} \mathbf{E}(x, y) = 0. \tag{1}$$

In most real cases, spatial variations of $\sigma(x, y)$ are caused mostly by variations of the 2D carrier concentration $n(x, y)$, which can be assumed throughout the whole paper by considering their mobility μ as a spatially-uniform constant. In this situation, with the help of the well-known current-field relationship in a magnetic field (see, e.g., [2]):

$$\mathbf{j} = \frac{en\mu}{1+\beta^2}\left[\mathbf{E} - \frac{\mu}{c}\mathbf{E}\times\mathbf{H}\right], \tag{2}$$

we can re-write the first of Eqs.(1) as

$$\operatorname{div}\left\{n(x, y)\left[\mathbf{E}(x, y) - \beta\mathbf{E}(x, y)\times\mathbf{h}\right]\right\} = 0 \tag{3}$$

where $\mathbf{h}$ is the unit vector in z-direction and $\beta = \mu H/c$ is the parameter of magnetic field strength.

It is impossible to obtain a general analytical solution of Eqs.(1) for an arbitrary $n(x, y)$, and we analyze this problem separately for the case of low ($\beta \ll 1$) and high ($\beta \gg 1$) magnetic fields.

2.1.1 Low magnetic field

For low magnetic field, the problem is solved by perturbations in β and therefore it is useful to begin with a brief description of the unperturbed state, that is with the general properties of conductivity of inhomogeneous

samples in the absence of magnetic field. The detailed description of different solvable models can be found in [1], and here we restrict ourselves to the most interesting case of random fluctuations of $n(x,y)$ with a very high amplitude, when maximal and minimal local values of $n(x,y)$ differ by at least several orders of magnitude. It will be always the case for non-degenerate electrons in a random inhomogeneities potential $V(x,y)$ with the dispersion $\Delta \gg kT$. In this case conductivity can be described in terms of the so-called percolation theory (see, e.g., [3, 4]) and is determined by n_p – carrier concentration at the percolation level V_p separating electron energies for which classical motion of electrons is finite and infinite:

$$\sigma_{xx} \simeq e n_p \mu. \tag{4}$$

Simple considerations [5, 6] show that for a symmetric random 2D potential $V(x,y)$, V_p coincides with the mean value $\overline{V(x,y)}$. We emphasize that this is a specific feature of 2D case, and for a 3D random potential, V_p lies essentially below $\overline{V(x,y)}$, differing from it by the value of order Δ (e.g., for a Gaussian 3D potential $V_p = \overline{V(x,y)} - 0.67\Delta$). Note that for both 2D and 3D-cases the percolation concentration n_p is essentially less than the average concentration in a sample $\overline{n(x,y)}$.

Now we return to the perturbation calculation of conductivity in the external magnetic field. The diagonal component of conductivity σ_{xx} is an even function of magnetic field and in the first order in β remain unchanged and given by Eq. (4). Much more interesting is the problem of σ_{xy}, which is absent at $H = 0$ and is determined by the linear in β terms. We denote by $\mathbf{E}_0(x,y)$ and $\mathbf{j}_0(x,y)$ the electric field and current density distributions in the absence of magnetic field. In low magnetic field they acquire additions $\mathbf{E}_1(x,y)$ and $\mathbf{j}_1(x,y)$ linear in β, related by the expression

$$\mathbf{j}_1(x,y) = e\mu n(x,y)\,[\mathbf{E}_1(x,y) - \beta \mathbf{E}_0(x,y) \times \mathbf{h}] \tag{5}$$

and meeting the equations

$$\operatorname{div} \mathbf{j}_1(x,y) = 0, \qquad \operatorname{curl} \mathbf{E}_1(x,y) = 0. \tag{6}$$

The boundary conditions for Eqs.(6) may be stated as the absence of current through the Hall contacts. After $\mathbf{E}_1$ is found, the Hall voltage may be calculated as $U_H = \int \mathbf{E}_1 d\mathbf{l}$ where the integration path goes from one Hall contact to the other.

In a homogeneous sample the solution of Eq. (5) and the first of Eq. (6) is

$$\mathbf{j}_1 = 0, \qquad \mathbf{E}_1 = \beta \mathbf{E}_0 \times \mathbf{h}. \tag{7}$$

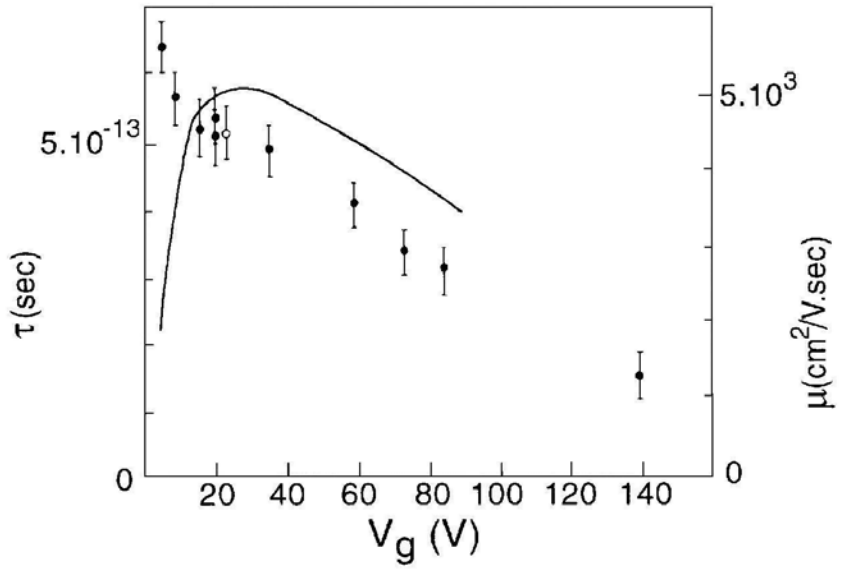

Figure 1: The relaxation time and mobility in a surface channel of MOS-transistor measured by the cyclotron resonance method [15]. The full line corresponds to the "Hall mobility" μ_H.

If this solution were correct also for an inhomogeneous sample, the Hall voltage could be determined by the formula [8]:

$$U_H = \frac{\beta}{e\mu} \int [\mathbf{j}_0(x,y) \times \mathbf{h}] \frac{d\mathbf{l}}{n(x,y)}. \tag{8}$$

However, the solution Eq. (7) is, generally speaking, incorrect for the inhomogeneous case, since it does not satisfy the second of Eq. (6). Note that in this case the integral in Eq. (8) does depend on the integration path. The latter circumstance reflects the well-known fact that in an inhomogeneous semiconductor the Lorenz force and the Hall field no longer locally compensate each other, so that the vortex current arise which were not taken into account in Eqs.(6). They flow near the boundaries between the regions with different carrier concentrations (Fig. 1), changing considerably the potential distribution in the high-resistive region and much less in the low-resistive one.

These facts lead to the following conclusion: the neglect of vortex currents and calculation of the Hall voltage by Eq. (8) is a good approximation

if the integration path in Eq. (8) is chosen so as to follow the way of minimal resistance, i.e. the percolation path in the Hall direction.

If the current density in the absence of magnetic field $\mathbf{j}_0$ were uniform, then one would obtain from Eq. (8) $U_H = \beta j_0 b/\sigma$ (b is the sample width). In this case, according to Eq. (4), the Hall coefficient $R_H = U_H/j_0 Hb$ would be $R_H \simeq (n_p ec)^{-1}$. But in fact, $\mathbf{j}_0(x, y)$ is strongly non-uniform. It is smaller in regions with low carrier concentration than in regions with high concentration. Due to this, the latter make a greater contribution to the integral for U_H than it would be at $\mathbf{j}_0 = \text{const}(\mathbf{r})$. As a result, the effective carrier concentration determined from the Hall effect: $n_H = (ecR_H)^{-1}$ in inhomogeneous samples exceeds the concentration at the percolation level n_c determining the conductivity:

$$n_H > n_p. \tag{9}$$

This important statement has a general character being valid for 3D inhomogeneities as well [1].

It is interesting to compare the results presented above for an arbitrary non-uniformity with the particular case of a two-phase metal-dielectric mixture where the problem allows an exact solution. It was shown more than half a century ago [7] that in 2D case dielectric inclusions does not change the Hall coefficient. The effect is due to the absence of vortex currents which cannot flow through dielectric. This means that n_H is exactly equal to n_m - the carrier concentration in the metallic phase. On the other hand, dielectric inclusions definitely decrease the sample conductivity resulting in the decrease of effective conductivity concentration below n_m, which again is in agreement with Eq. (9).

The inequality Eq. (9) has a very serious consequence related to the interpretation of experimental galvanomagnetic data in inhomogeneous samples. It is well known that in uniform samples the product $c\sigma_{xx}R_H \equiv \mu_H$ called Hall mobility is equal to the real drift mobility μ (sometimes with an additional factor not much differing from 1) and represents the most simple and popular method of mobility measurements. We see from Eq. (9) that in non-uniform samples μ_H is no longer equal to the carrier mobility and always

$$\mu_H < \mu. \tag{10}$$

For very large Δ – inhomogeneity amplitude, n_H and n_p and, hence, μ_H and μ may differ by orders of magnitude. If we accept that for non-degenerate electrons spatial fluctuations of concentration are determined by the factor $\exp(\Delta/kT)$, then it becomes evident that the difference between n_H and

n_p and, hence, the ratio μ/μ_H increases with the temperature decrease. Therefore, for a fixed inhomogeneity amplitude the μ_H value will sharply drop at low temperature. Such anomalous temperature dependence of μ_H has nothing in common with a weak temperature dependence of μ different for different scattering mechanisms.

As we have already mentioned, the anomalous temperature dependence of "Hall mobility" μ_H is a phenomenon realized in both 3D and 2D electron systems. There exist a very large number of experimental works where this effect was observed (partially cited in [1]) most of which were performed on bulk 3D semiconductor samples. It has a simple explanation. Inhomogeneities are usually observed in heavily doped and strongly compensated, irradiated, or polycrystalline semiconductors [1], in other words, in materials with high concentration of defects or impurities and, hence, with relatively low mobility. On the other hand, for observation of size quantization in 2D electron gas the quantization energy is required to exceed the energy uncertainty caused by scattering, which is impossible at very low carrier mobility. Thus many structures containing inhomogeneities do not satisfy the conditions of two-dimensionality and hence are not used for detailed investigations.

Nevertheless, we can point at a number of experimental observations of the described μ_H anomaly in 2D systems, first of all, in inverse channels of Si MOS-transistors (see, e.g., [9–13]). The effect always strongly depended on the gate voltage V_g disappearing at large V_g corresponding to a strong inversion. This is easily explained by the fact that the growing number of inversion carriers, on the one hand, screened inhomogeneities decreasing their amplitude and, on the other hand, raised the Fermi level above the maxima of potential fluctuations making their influence negligible. It should be noted that the strong temperature and V_g dependence of μ_H in many cases could be also explained by an alternative concept [14] connecting this effect with the Mott-Anderson transition, or localization of single electrons in microscopic potential fluctuations. Of course, these processes may take place and in some cases decrease the real mobility in MOS channels. But the conductivity at the transition point (gate voltage corresponding to the offset of exponential temperature dependence of μ_H) varied in experiments and differed considerably from the universal Mott value of minimal metallic conductivity $0.07e^2/\hbar$ [15]. This fact contradicted the microscopic localization concept and led the authors of [16] to the conclusion about the important role of large-scale potential fluctuations, that is, in fact, to the model discussed above.

The most impressive argument in favour of this model is the result of

high-frequency measurements [17] shown in Fig. 1. It is seen that the sharp decrease of μ_H at low V_g (accompanied by anomalous temperature dependence) is not reproduced in the behaviour of high-frequency mobility, which means that it is not connected with the properties of a real mobility and is rather due to the inhomogeneity effect.

To conclude, we mention briefly some special model experiments [18] in MOS structures with a multi-connected electrode of a chessboard shape. The potential of the "black" and "white" checks of the "chessboard" and, hence, the carrier concentration underneath could be varied independently. Therefore, the degree of a surface channel inhomogeneity was manually operated. The conductivity and Hall effect were measured at different inhomogeneity levels. The results confirm the basic conclusion that any concentration inhomogeneity decreases the experimentally measured μ_H which in an inhomogeneous sample have nothing in common with the real surface mobility determined by the scattering effects in the inversion channel.

So far in this section we have considered linear in β effects determining the Hall effect and non-diagonal conductivity component σ_{xy}. Quadratic in β terms are responsible for the changes of σ_{xx} in magnetic field (magnetoresistance). We remind that in uniform samples magnetoresistance is due to the dependence of momentum relaxation time τ on the energy of electrons and can be written as

$$-\frac{\Delta\sigma_{xx}}{\sigma_{xx}} = \frac{\Delta\rho}{\rho_0} = B\beta^2 \tag{11}$$

where ρ_0 is the zero-field resistivity of the sample, $\Delta\rho$ is its change is magnetic field and numerical factor B depends on the scattering mechanism. It is equal to 2.155 for impurity scattering, to 0.38 for deformation acoustic phonon scattering and vanishes if τ is independent of energy.

To find $\Delta\sigma_{xx}$ in non-uniform samples, we take into account that at very large amplitude of inhomogeneity the sample resistance is determined by saddle points of the random potential $V(x, y)$ with the energy close to the percolation level V_p. It is natural to suppose that the magnetoresistance will be associated with the field dependence of the saddle point resistances. Let us calculate the magnetoresistance of a single saddle point, which is a point where $\partial V/\partial\xi = 0$ ($\xi = x, y$), whereas two second derivatives $\partial^2 V/\partial\xi^2$ have different signs. The concentration distribution near such a point is:

$$n(x, y) = n_0 \exp\left(\frac{x^2}{l_x^2} - \frac{y^2}{l_y^2}\right) \tag{12}$$

where $l_\xi^2 = 2kT\left|\frac{\partial^2 V}{\partial\xi^2}\right|_0^{-1}$, index 0 refers to the saddle point and the x-axis

is chosen along the current flow. The external voltage U applied along this axis causes some distribution of potential $\varphi(x,y)$ and current density $\mathbf{j}(x,y)$ around the saddle point. To determine them, we shall use a standard expression for current distribution in a magnetic field, which in the lowest orders in β has the form

$$\mathbf{j}(x,y) = e\mu n(x,y)\left[-\nabla\varphi(x,y)\left(1-\beta^2\right) + \beta\nabla\varphi(x,y)\times\mathbf{h}\right]. \qquad (13)$$

(By retaining only the first-order terms, Eq. (13) gives the above-used expression Eq. (5)).

For the expressions Eqs.(12),(13), the basic equation $\operatorname{div}\mathbf{j} = 0$ acquires the form

$$\frac{\partial^2\varphi}{\partial x^2} + \frac{\partial^2\varphi}{\partial y^2} + \frac{2x}{l_x^2}\frac{\partial\varphi}{\partial x} - \frac{2y}{l_y^2}\frac{\partial\varphi}{\partial y} + \frac{2x}{l_x^2}\beta\frac{\partial\varphi}{\partial y} + \frac{2y}{l_y^2}\beta\frac{\partial\varphi}{\partial x} = 0. \qquad (14)$$

We must solve this equation with the boundary condition $\varphi(x=\infty) - \varphi(x=-\infty) = U$. The solution gives

$$\begin{aligned}\varphi(x,y) &= \frac{U}{\sqrt{\pi}}\int_{-\infty}^{x/l_x}\exp(-t^2)dt + \frac{U\beta y l_x}{\sqrt{\pi}(l_x^2+l_y^2)}\exp\left(-\frac{x^2}{l_x^2}\right)\\ &+\frac{U\beta^2 x l_x(l_y^2-2y^2)}{2\sqrt{\pi}(l_x^2+l_y^2)^2}\exp\left(-\frac{x^2}{l_x^2}\right). \qquad (15)\end{aligned}$$

Substitution of Eq. (12) and Eq. (15) into Eq. (13), followed by integration over y, gives us the full current through the saddle point J_x and hence the resistance $R = U/J_x$. More thorough analysis of the problem was performed in [1, 19]. It takes into account the fact that, due to the dependence of carrier mobility μ on their energy E (which usually has a power character: $\mu \sim E^\alpha$), the parameter β is different for different carriers and additional averaging with the Boltzmann distribution function for carriers is required. Precise calculations result in the formula similar to Eq. (15) where the second and the third terms have additional numerical factors

$$a_1 = \frac{3\sqrt{\pi}\Gamma(2\alpha+5/2)}{4\Gamma^2(\alpha+5/2)} \text{ and } a_2 = \frac{9\pi\Gamma(3\alpha+5/2)}{16\Gamma^2(\alpha+5/2)}.$$

The final result of calculations is the formula for a relative magnetoresistance of a saddle point

$$\frac{\Delta R}{R} = \beta^2\left(a_2 - \frac{a_1^2}{2}\right). \qquad (16)$$

This formula does not depend on the saddle point parameters n_0, l_x, l_y and, therefore, it applies to all saddles. Hence, it follows that the magnetoresistance of a whole sample is also described by Eq. (16). By comparing Eq. (11) and Eq. (16), we conclude immediately that in strongly inhomogeneous samples the magnetoresistance coefficient $B = \left(a_2 - \frac{a_1^2}{2}\right)$.

The most important conclusion consists in the fact that, contrary to uniform samples, magnetoresistance exists even in the absence of energy dependence of the scattering time. For $\alpha = 0$, when in uniform samples $B = 0$, Eq. (16) immediately gives $B = 0.5$. Such a magnetoresistance, usually called "geometric" to distinguish it from the standard, "physical" one, has a simple explanation. Any magnetoresistance occurs when the Lorenz force and the Hall electric field influencing moving carriers, compensate each other only on average but not at the level of each individual carrier so that their trajectories become slightly bent in one or another side decreasing the total current. For the "physical" mechanism it is due to the dispersion of the Hall angle for carriers with different energy while for the "geometric" mechanism it is due to shorting of the Hall field by low-resistive regions of an inhomogeneous sample. For $\alpha \neq 0$ both mechanisms act together so that the "geometric" factor increases B from 2.155 to 4.02 for impurity scattering and from 0.38 to 1.07 for deformation acoustic phonon scattering.

2.1.2 High magnetic field

We begin with the Hall effect in classically high magnetic field ($\beta \gg 1$) in a non-uniform sample. We can no longer use the perturbation approach and, instead of Eq. (5) for the magnetic field-induced addition to the current, we have the following approximate expression for the whole current

$$\mathbf{E}(x, y) = \frac{\beta}{e\mu n(x, y)} [\mathbf{j}(x, y) \times \mathbf{h}] \tag{17}$$

where we have restricted ourselves to the highest order term in β. Requiring curl $\mathbf{E}$ =0,we obtain immediately [20]

$$\mathbf{j}(x, y) \cdot \operatorname{grad} n(x, y) = 0. \tag{18}$$

This means that the current tends to flow along the equipotential lines of inhomogeneity potential $V(x, y)$. It is interesting that some qualitative considerations concerning such current behaviour were already put forward long ago [21] and then used anew in connection with the theory of quantum Hall effect [22, 23]. We should emphasize that this very important statement

concerns only the 2D case and is not correct for 3D inhomogeneities. It should be noted that the mentioned 2D case does not mean necessarily 2D electron gas. It may be also a bulk semiconductor where the inhomogeneity potential does not depend on one of the coordinates (for instance, a system of parallel dislocations) and the magnetic field is oriented along this coordinate.

For two-phase systems, Eq. (18) means that in high magnetic field n_H is determined by the carrier concentration in the connected phase (in the 2D case, contrary to the 3D one, there is always one connected phase. For a statistical mixture it will be the phase with a relative volume $C > 0.5$. It is worth noting that in a metal-dielectric mixture (and only in it!) this conclusion is valid also at low fields, as it was mentioned in Sect. 2.1.1.

In semiconductors with a random inhomogeneity potential, the Hall effect will be determined by the carriers in those sample regions where the band edge lies in a narrow energy strip near V_p. This means that $n_H \simeq n_p$. From the non-connected regions with both $n \gg n_p$ and $n \ll n_p$, the current lines are forced out by high magnetic field. As a result, anomalous small magnitude and strong temperature dependence of the "Hall mobility" μ_H, typical for inhomogeneous samples in a low magnetic field, should not be observed in a high field. The Hall coefficient must increase with the magnetic field from $R_H \simeq (ecn_H)^{-1}$ to $R_H \simeq (ecn_p)^{-1}$.

If we want to know not only the Hall coefficient but the magnetoresistance as well, we cannot use Eq. (17) containing only the non-dissipative term with $\mathbf{j} \perp \mathbf{E}$ and thus unable to describe diagonal (dissipative) conductivity component σ_{xx}. To find it, we use the same approach as in Sect. 2.1.1 considering magnetoresistance of one single saddle point of inhomogeneity potential Eq. (12) but with Eq. (13) replaced by its high-field analog

$$\mathbf{j}(x,y) = e\mu n(x,y)\left[-\nabla\varphi(x,y)\beta^{-2} + \beta^{-1}\nabla\varphi(x,y)\times\mathbf{h}\right] \tag{19}$$

(Eq. (17) corresponds to the last term of this expression). It gives absolutely the same equation for the potential Eq. (14) as in the low-field case. However, its approximate solution will be different since in Sect. 2.1.1 we found the lowest terms of expansion by β while here, on the contrary, we are interested in the highest degrees of β.

We assume the solution to have the form

$$\varphi(\zeta,\eta) = \varphi_0(\zeta) + \exp(-\zeta^2)\sum_{n=1}^{\infty}\beta^n\sum_{i,j}\alpha_{ij}^{(n)}\mathrm{H}_i(\zeta)\mathrm{H}_j(\eta) \tag{20}$$

where $\zeta = x/l_x$, $\eta = y/l_y$, H_i are the Hermite polynomials and

$$\varphi_0(\zeta) = \frac{U}{\sqrt{\pi}} \int\limits_{-\infty}^{\zeta} \exp(-t^2)dt$$

is the solution in the absence of magnetic field (the first term of Eq. (15)).

Substitution of Eq. (20) into Eq. (14) transforms the latter into a complicated infinite set of algebraic equations. But we do not need to determine all coefficients $\alpha_{ij}^{(n)}$. Due to orthogonality of the Hermite polynomials, only terms with $i = 0$ and $j = 1$ will contribute to the total current across the saddle point

$$J_x = \frac{\sqrt{\pi} e\mu n_0}{\lambda\beta^2} U \exp(\zeta^2) \int\limits_{-\infty}^{\infty} \left[\frac{\partial\varphi}{\partial\zeta} + \lambda\beta\frac{\partial\varphi}{\partial\eta}\right] \exp(-\eta^2)d\eta \qquad (21)$$

($\lambda = l_x/l_y$). Therefore, we restrict ourselves to determination of the above coefficients. This is not a very difficult procedure [24] , which gives

$$\begin{aligned} J_x &= \frac{\sqrt{\pi} e\mu n_0}{\lambda\beta^2} U \left\{1 + \frac{\lambda^2\beta^2}{1+\lambda} \sum_{k=0}^{\infty} (-1)^k \frac{(2k)!}{(k!)^2} \left[\frac{\lambda\beta^2}{(1+\lambda^2)^2}\right]^k\right\} \\ &= \frac{\sqrt{\pi} e\mu n_0}{\lambda\beta^2} U \left\{1 + \frac{\lambda^2\beta^2}{\sqrt{(1+\lambda^2)^2 + 4\lambda\beta^2}}\right\}. \end{aligned} \qquad (22)$$

A macroscopic sample contains a large number of saddle points and its equivalent electric scheme is a random network of resistors, each of which is characterized by a set of parameters: n_0, l_x, l_y. At $\Delta/kT \gg 1$ the range of resistor values is determined mainly by n_0 fluctuations and, to a lesser degree, by fluctuations of $l_{x,y}$. It allows us to average Eq. (22) over $l_{x,y}$. As to n_0, one sees that the relative magnetoresistance $\Delta R/R$ of a saddle point is n_0 -independent and, in average, the same for all saddle points. Therefore, this quantity determines also the relative magnetoresistance of the sample as a whole, for $\beta \gg 1$ equal to

$$\frac{\Delta\rho}{\rho_0} \simeq 2\beta. \qquad (23)$$

Thus the magnetoresistance of inhomogeneous semiconductors in strong magnetic fields is characterized by a qualitatively new phenomenon. Magnetoresistance at high magnetic fields increases linearly with the field, contrary to homogeneous samples where $\Delta\rho/\rho_0$ saturates at high magnetic fields.

2.1.3 Extremely high magnetic field

In uniform samples, two limiting cases $\beta \ll 1$ and $\beta \gg 1$ considered above exhaust all principal possibilities, which can be realized in the absence of Landau quantization. In non-uniform samples, one more large parameter emerges, namely, the typical concentration ratio for different saddle points $n_{0\,\max}/n_{0\,\min}$. The calculations of Sect. 2.1.2 are valid only if this parameter is larger than β, or at not very high magnetic fields. In the opposite limit the magnetic field may cause considerable redistribution of the current along different saddle points. Due to this redistribution we cannot assume, as before, the net relative magnetoresistance to be equal to that for a single saddle point. The situation requires some other approach.

This problem was solved by Dreizin and Dykhne [25]. They elaborated a special diagrammatic technique for calculation of conductivity in inhomogeneous media in extremely high magnetic fields when β is the largest parameter of the system. However, their main qualitative result can be obtained using fairly simple physical considerations, which are reproduced below.

Since the tensors of conductivity and diffusion coefficients are proportional to each other, it is more reasonable to speak about electron diffusion in the constant magnetic field $\mathbf{H} \parallel \mathbf{z}$ and random electric fields of inhomogeneities $E \sim \Delta/eL$, rather than about conductivity. Diffusion in the xy-plane is strongly suppressed $\sim \beta^{-2}$ by the magnetic field and the main transport here will be due to the Hall drift with the typical velocity $v \sim c\Delta/eHL$ in random fields. Thus we can imagine the electron motion as a sequence of random walks where a particle moves with the velocity v and after covering the distance $\sim L$ randomly changes its direction. Using the well-known estimate of the diffusion coefficient D for random walks, we have

$$D \sim vL \sim \frac{c\Delta}{eH}. \tag{24}$$

It is interesting to note that D depends only on the amplitude but not on the spatial size of the inhomogeneity potential.

We see that the diffusion coefficient, which is proportional to the diagonal component of conductivity σ_{xx}, is $\sim H^{-1}$. Since the non-diagonal component $\sigma_{xy} \sim H^{-1}$, we may finally conclude that the resistivity $\rho_{xx} = \sigma_{xx}/(\sigma_{xx}^2 + \sigma_{xy}^2)$ and, hence, the magnetoresistance do not saturate but grow linearly in high magnetic fields, similarly to Eq. (23) but with another proportionality factor. This differs from the case of 3D inhomogeneities where Eq. (23) remains valid but in the situation described in the present section, $\rho_{xx} \sim H^{2/3}$ [1, 25].

2.2 Hall-induced edge charges

So far we have considered galvanomagnetic phenomena in 2D samples with built-in concentration inhomogeneities, which can be caused by different technological reasons. However, even ideally uniform samples in the conditions of Hall effect acquire some specific inhomogeneity having a very simple explanation. The Lorenz force affecting moving carriers in a magnetic field causes their shift in the Hall direction creating, in turn, the Hall electric field. As a result, one half of the sample becomes enriched and the other – depleted by carriers creating a gradient of concentration n and of chemical potential ζ perpendicular to the current [26]. This effect has a general character but in bulk samples is usually negligible: the deviations from neutrality occur only in surface layers with the thickness of order of the screening radius, and the change in ζ is very small in comparison to the applied voltage. In 2D samples the situation changes dramatically. We will show that, due to much weaker screening in low-dimensional systems (see, e.g., [27]), nonuniformities of carrier density and electric field exist throughout the whole sample and acquire noticeable values subjected to direct experimental determination.

Let us assume that we apply the external voltage U and pass the current in x-direction. Our theoretical analysis will be based on the equation

$$\sigma_{xx}^0 \left(-\frac{\partial \varphi}{\partial y} + \frac{1}{e}\frac{\partial \zeta}{\partial y} \right) + \sigma_{xy}^0 \left(-\frac{\partial \varphi}{\partial x} + \frac{1}{e}\frac{\partial \zeta}{\partial x} \right) = 0 \tag{25}$$

expressing the absence of Hall current j_y. The superscript 0 in conductivity is intended to emphasize the fact that, contrary to the previous sections, we consider samples with uniform carrier concentration. We will assume that the sample length in the direction of the current L is much more than the width b in the Hall direction, which is typical for the samples for Hall measurements. In this case the above-mentioned concentration inhomogeneity far from the current contacts will depend only on the y-coordinate and we simplify Eq. (25) by assuming $\partial\zeta/\partial x = 0$ and $\partial\varphi/\partial x = -E_x = U/L = \mathrm{const}(\mathbf{r})$.

If the carrier density fluctuations $n(y) - n_0$ (n_0 is the equilibrium electron density equal to the non-compensated impurity concentration) are not large, we can expand ζ in terms of $n - n_0$: $d\zeta/dy = (d\zeta/dn)_0 dn/dy$ ($(...)_0$ means the value calculated at $n = n_0$) and write Eq. (25) in the form

$$\frac{\partial \varphi}{\partial y} = \frac{1}{e}\left(\frac{d\zeta}{dn}\right)_0 \frac{dn}{dy} + \beta E_x. \tag{26}$$

We have taken into account that $\sigma^0_{xy} = \beta\sigma^0_{xx}$.

To find the potential distribution, Eq. (25) should be complemented with one more equation connecting φ and ζ or, in other words, describing the screening phenomena in a sample. In 3D systems it is the Poisson equation with the right side describing the electron charge in terms of ζ. In 2D systems the description of screening phenomena is essentially different [27]. The electric field created by some charge separation exists in the whole 3D space while the charge of screening electrons is confined to the plane of 2D gas. That is why the potential is described not by the Poisson, but by the Laplace equation $\partial^2\varphi/\partial y^2 + \partial^2\varphi/\partial z^2 = 0$ in the half-space $z > 0$ above the 2D gas. All the screening phenomena are hidden in the boundary condition

$$\frac{\partial\varphi}{\partial z}(y,0) = 2\pi e\left[n(y) - n_0\right]. \tag{27}$$

Assuming $\varphi(0,0) = 0$, we obtain by integrating Eq. (26) that

$$\varphi(y,0) - \beta E_x y = \frac{1}{e}\left(\frac{d\zeta}{dn}\right)_0 \left[n(y) - n_0\right] \tag{28}$$

which, after substituting into Eq. (27), given eventually the boundary condition for φ:

$$\frac{\partial\varphi}{\partial z}(y,0) = \begin{cases} l_2^{-1}\left[\varphi(y,0) - \beta E_x y\right], & |y| \le b/2; \\ 0, & |y| > b/2. \end{cases} \tag{29}$$

Here $l_2 = (d\zeta/dn)_0/(2\pi e^2)$ is the 2D screening length. For a degenerate 2D electron gas, l_2 is equal to half of the effective Bohr radius a_B, and the expressions Eqs.(28),(29) are valid not only for small but for any Δn, which results from the constant density of states in 2D electron gas.

The Laplace equation with the boundary condition Eq. (29) resembles that of the theory of contact phenomena in 2D electron gas [27] and some conclusions can be made *a priori* by analogy. The screening capability of 2D electrons is much weaker than in the bulk sample and any charge inhomogeneity will decrease very smoothly with the logarithmic divergence of the total screening charge. As a result, rather large effects can be observed even for samples with $b \gg l_2$.

The equation cannot be solved analytically but can be transformed to an integral equation more convenient for numerical solution. We will operate in terms of dimensionless units:

$$\xi = y/l_2, \qquad \eta(\xi) = \frac{2\pi e}{\beta E_x}[n(y) - n_0], \qquad \psi(\xi) = \frac{\varphi(y,0)}{l_2\beta E_x}.$$

In these units the solution of the Laplace equation with the boundary conditions Eq. (29) is

$$\psi(\xi) = -\frac{2}{\pi}\int\limits_0^\infty \sin(\lambda\xi)\exp(-\lambda z/l_2)\frac{d\lambda}{\lambda}\int\limits_0^{b/2l_2}\eta(\xi')\sin(\lambda\xi')d\xi'. \qquad (30)$$

Assuming $z = 0$ and substituting Eq. (30) into Eq. (29), we obtain

$$\nu(\xi) = -\frac{2}{\pi}\int\limits_0^\infty \sin(\lambda\xi)\frac{d\lambda}{\lambda}\int\limits_0^{b/2l_2}\eta(\xi')\sin(\lambda\xi')d\xi' - \xi. \qquad (31)$$

After integration over λ we have the final form of the integral equation:

$$\eta(\xi) = -\frac{1}{\pi}\int\limits_0^{b/2l_2}\eta(\xi')\log\left(\frac{\xi+\xi'}{|\xi-\xi'|}\right)d\xi' - \xi. \qquad (32)$$

This equation can be easily solved numerically, which gives us the concentration distribution along the Hall direction for 2D stripes of different widths b. After $\eta(\xi)$ is found, the potential distribution $\psi(\xi)$ and the Hall voltage $\psi(b/2l_2) - \psi(-b/2l_2)$ are determined by Eq. (30). Some of the final results are shown in Fig. 2 demonstrating the distributions of the electron concentration and the electrostatic potential in a structure with $b = 20l_2$. The most remarkable feature here is the non-monotonic character of $\psi(\xi)$ (that is of $\varphi(y, 0)$), which means the change of electric field sign near the sample edges. Noticeable deviations from neutrality are seen at fairly large distance from the edges. Calculations also show that, contrary to the 3D case, the difference in electron concentrations at opposite edges does not saturate at large b, increasing approximately $\sim b^{1/2}$. To explain this fact, we note that far from the sample edge one can neglect the diffusion current (the first term on the right-hand side of Eq. (26)). In this approximation the function $\psi(\xi)$ is linear while the charge density diverges near the edge:

$$\eta(\xi) \simeq -\frac{2\xi}{\sqrt{b^2/l_2^2 - 4\xi^2}} \qquad (33)$$

(see, e.g., [28]). The diffusion term will provide an effective screening constraining the concentration increase at the distance $\sim l_2$ from the edges. As a result, the charge density near the edge is of order $(b/l_2)^{1/2}(\beta E_x/2\pi e)$.

The problems related to experimental observations of the Hall-induced edge charges will be discussed later in Sect. 3.3.

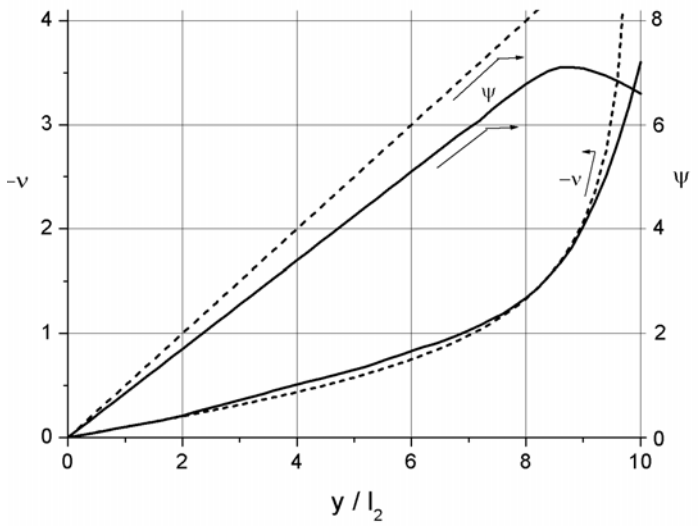

Figure 2: Coordinate dependence of the dimensionless charge density η (left scale) and dimensionless Hall potential ψ (right scale) in 2D electron gas with $b/l_2 = 20$ [26]. The broken lines show these values in the absence of electrostatic effects ($l_2 \to 0$).

3 Quantizing magnetic field

Now we turn to the case of 2D electron gas in a perpendicular quantized magnetic field. In this situation electrons acquire pure discrete energy spectrum representing a system of equidistant Landau levels (LLs): $E_N = (eH/mc)(N + 1/2) \equiv \hbar\omega_c(N + 1/2)$ $(N = 0, 1, 2, ...)$, each of them is degenerate $\nu \equiv eH/(\pi\hbar c)$ times per unit area. These specific features – discreteness and degeneracy – of the energy spectrum modify dramatically all electronic properties resulting in a number of new phenomena, the most famous of which is the quantum Hall effect. Quantization of energy spectrum also seriously modify galvanomagnetic phenomena in non-uniform samples considered in Sect. 2 for a classical electron gas.

3.1 Screening in quantum Hall systems

Prior to analyzing galvanomagnetic phenomena in non-uniform quantum Hall

systems, we consider the general question of how the quantizing magnetic field modifies spatial distribution of 2D electrons $n(x, y)$ in an inhomogeneous potential $V(x, y)$, which in the classical case is locally connected to $V(x, y)$ by the Fermi (or Boltzmann) function. Due to a singular character of the density of states, quantized electron gas can no longer provide local connection between potential and concentration. First of all, we illustrate it qualitatively and present a general picture of screening in quantum Hall systems [26, 29] assuming a degenerate character of 2D electron gas.

Let us consider one-dimensional band bending $V(x)$, created, for instance, by some depleting external potential. If we, for a moment, neglect the self-consistent potential created by electrons, then the electron density distribution $n(x)$ would have a stepwise distribution shown in Fig. 3. At each point where some LL crosses the Fermi level ζ_0, $n(x)$ changes abruptly by ν. If now we remember that electrons are charged particles, then such a singular behaviour of electron density on the background of a uniform or slowly varying density of compensating impurity change will mean the presence of charged strips dramatically deforming the bare potential. Instead of steps in electron density, we obtain a self-consistent potential φ containing horizontal plateaus with ζ_0 pinned to some LL (Fig. 3).

As a result, in the presence of a non-uniform potential, 2D electron gas in quantizing magnetic fields becomes separated into a series of alternating regions of two different types:

1. "metallic", or "compressible" regions where the local filling factor is non-integer, ζ_0 coincides with some LL, electron concentration varies along the region differing by ν at opposite edges of the same layer but in equilibrium electrical potential remains constant;

2. "dielectric", or "incompressible" regions where the local filling factor is integer, ζ_0 lies is a gap between LLs, electron concentration remains constant equal to νN $(N = 0, 1, 2, ...)$ but potential varies differing by $\hbar\omega_c/e$ at opposite edges of the same layer.

We will calculate the distribution of concentration and potential inside "metallic" and "dielectric" regions and the widths of these regions assuming one-dimensional character of inhomogeneities when n depends only on the x-coordinate and φ – only on x and z. As any screening problem in

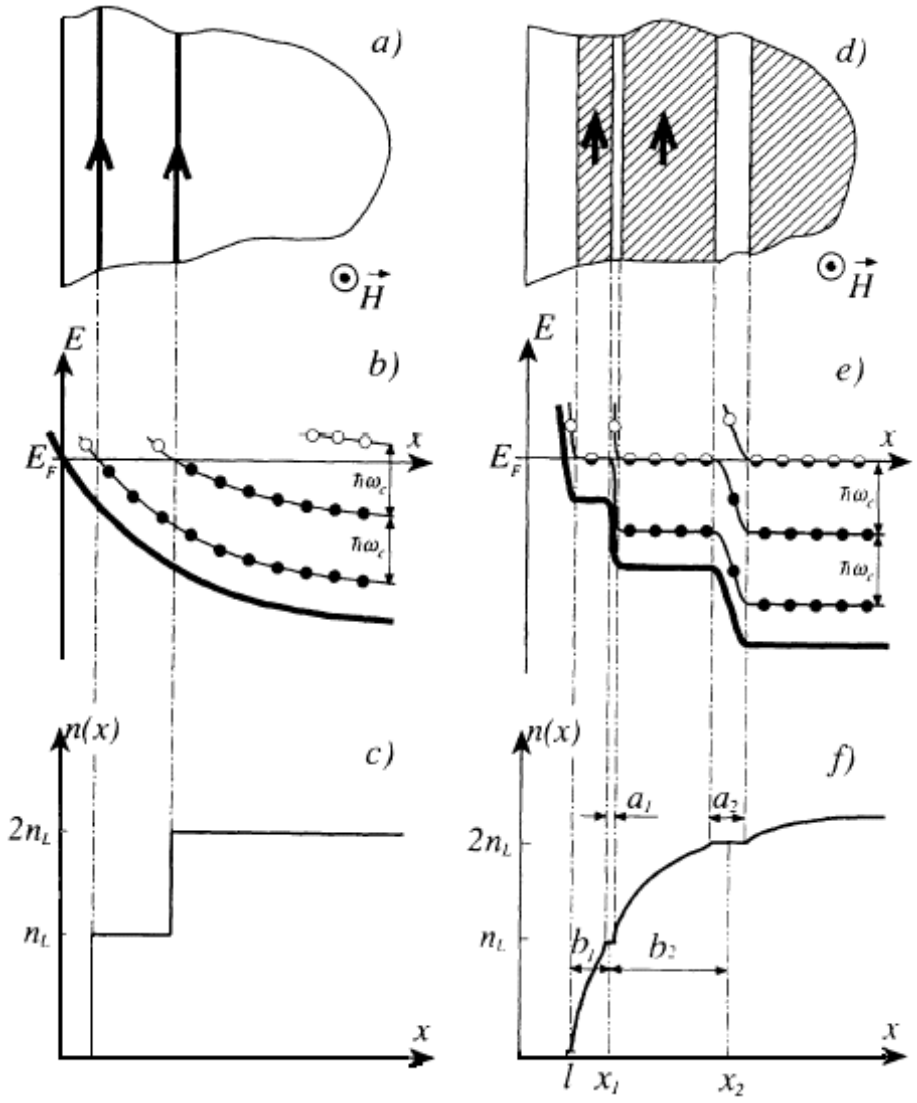

Figure 3: Non-uniform 2D gas in quantizing magnetic field [29]. (a)-(c) – one-electron picture. (a) – top view of 2D electron gas. (b) – bending of LLs. (c) – coordinate dependence of the electron density. (d)-(f) – self-consistent electrostatic picture. (d) – top view of 2D electron gas; shaded strips represent "metallic" regions with non-integer filling factor, unshaded strips represent "dielectric" integer filling factor regions. (e) – bending of the potential energy and the LLs. (f) – coordinate dependence of the electron density. Circles in (b) and (e) represent local filling of the LLs.

a 2D gas (see Sect. 2.2), this calculation consists in solving the Laplace equation $\partial^2\varphi/\partial x^2 + \partial^2\varphi/\partial z^2 = 0$ outside the plane containing electrons, with corresponding boundary conditions on this plane. Following [29], we will assume for simplicity that 2D electron gas is formed at the surface of a semiconductor with high dielectric constant $\varepsilon \gg 1$ so that almost all electric field surrounding the structure is concentrated in vacuum above it, that is at $z > 0$.

Particular solutions will be obtained for two different problems: the quantum Hall system with non-uniform doping and the Hall-induced charge inhomogeneity (the problem similar to Sect. 2.2 but for the case of quantizing magnetic field). The solution of one more similar problem – edge states caused by a potential barrier at the sample edge – can be found in the original paper [29].

3.2 Non-uniform doping

Let our sample have a non-uniform profile of doping level $n_0(x, y)$, smooth enough to fulfil conditions of quasi-neutrality and assume that the equilibrium 2D electron concentration in zero magnetic fields is given by the same function. For simplicity of calculations, we will assume that the compensating positive charge lies in the same plane as 2D electrons. Generalization to the case of modulation-doped or MOS-structures has no principal difficulties.Quantizing magnetic field may result in re-distribution of electron concentration and deviation from local neutrality near the lines where local n_0 values are close to νN (integer filling factors). At $T \to 0$ the Fermi level at both sides of these lines should be pinned to different LLs requiring a potential step of the height $\hbar\omega_c$. To form such a junction, some carriers from the upper, $(N + 1)$ -st LL in the region of higher concentration cross the line and move to the empty places at the N-th level, creating a charged dipole strip.

To calculate parameters of this strip, we place the origin at some point of the line $n_0 = \nu N$ and direct the x-axis along the gradient of n_0. This allows us to consider concentration distribution as depending only on x (if the curvature of equiconcentration lines is not very large). By expanding n_0 near the origin: $n_0(x) = \nu N + \alpha x$ we can obtain a relatively simple system of boundary conditions for the Laplace equation determining the potential distribution above the $z = 0$ plane. If l is the width of depletion region abandoned by electrons from the $(N + 1)$-st LL (to be found below), then the surface charge density in the region $-l < x < l$ will be $e\alpha x$. Outside this region the Fermi level is pinned to the corresponding LLs and potential in

the layer is constant. This results in the following boundary conditions for $\varphi(x,z)$:

$$\begin{aligned} \varphi(x,z &= 0) = 0, \qquad x < -l; \\ \frac{\partial\varphi}{\partial z}(x,z &= 0^+) = -4\pi e\alpha x, \qquad -l < x < l; \\ \varphi(x,z &= 0) = \hbar\omega_c/e, \qquad x > l. \end{aligned} \tag{34}$$

Such a problem with the character of boundary conditions changing along the x-axis, can be solved either by conformal transformations [30] or by means of analytic functions theory [29]. The answer for the potential profile in a "dielectric" region $-l < x < l$ is

$$\varphi(x,0) = \frac{\hbar\omega_c}{2e}\left(\frac{2\arcsin(x/l)}{\pi} + 1\right) + 2\pi e\alpha x\sqrt{l^2 - x^2}. \tag{35}$$

Both terms in Eq. (35) contain square-root singularities in the electric field $E_x = -\partial\varphi/\partial x$ at $x = \pm l$. Since real potential has no singularities, we must require these terms to cancel each other, which gives us the expression for l:

$$l = \frac{1}{\pi e}\sqrt{\frac{\hbar\omega_c}{2\alpha}}. \tag{36}$$

Similarly, we can find the distribution of charge density

$$\sigma(x) = -(4\pi)^{-1}\frac{\partial\varphi}{\partial z}(x, z = 0^+)$$

in "metallic" regions $|x| > l$. We restrict ourselves to its asymptotic for $x \gg l$, which is

$$\sigma(x) \simeq \frac{\hbar\omega_c}{4\pi^2 ex}. \tag{37}$$

Note that this expression with a very slow decrease of charge density is a universal law, typical for a screened potential in a 2D electron gas [27] and independent of the presence and magnitude of magnetic field (the presence of ω_c in the formula marks only the amplitude of potential to be screened but not the influence of a field on the screening itself). As a result, the total positive and negative charges, as well as the dipole moment of the strip diverge. Physically, it means that even at large distance between strips, they cannot be treated independently.

The most important conclusion from the above is the presence of dipole strips even at very small amplitude of concentration fluctuations Δn_0. If $\Delta n_0 \ll \nu$, then such strips occur only at the average filling factor close to an integer. Thus we may expect some additional features in Shubnikov-de Haas-like oscillations of different characteristics of quantum Hall systems in the vicinity of integer filling factors.

3.3 Hall-induced edge charges

Now we are returning to the problem of Hall-induced edge charges considered in Sect. 2.2 for classical magnetic fields in order to discuss modifications of this effect in the presence of quantized magnetic field changing dramatically the electron screening processes. We analyze this problem for two qualitatively different situations depending on the equilibrium Fermi level position ζ_0 [26].

Let us discuss first the situation when the electron concentration in equilibrium n_0 and the magnetic field H have such values that n_0/ν have a non-integer value or, in other words, ζ_0 in the middle of the sample coincides with some LL: $\zeta_0 \simeq \hbar\omega_c(N+1/2)$ and does not depend on the concentration. In this region Eq. (28) gives directly

$$\varphi(y,0) = \beta E_x y. \tag{38}$$

But this cannot be the case across the whole sample since, according to Eq. (33), it would require infinite charge density near the edges (formally this results from the definition of l_2 which becomes zero owing to infinite density of states at a LL). Therefore, for any applied voltage there will be "dielectric" strips near the edges. To find the width of these strips δ, as well as the exact potential and charge density distribution in the sample, we again solve the Laplace equation but with different boundary conditions than in our previous problems. Assuming for illustration purposes the case of half-filled LL in the bulk, we have

$$\begin{aligned} \varphi(y,z &= 0) = \beta E y, \qquad 0 < y < b/2 - \delta; \\ \frac{\partial\varphi}{\partial z}(y,z &= 0^+) = 2\pi e\nu, \qquad b/2 - \delta < y < b/2; \\ \frac{\partial\varphi}{\partial z}(y,z &= 0^+) = 0, \qquad y > b/2 \end{aligned} \tag{39}$$

and antisymmetric potential shape at negative y. Instead of applying conformal transformation, we use here another approach and transform the Laplace equation into the integral equation for the charge density $\sigma(y)$ in the "metallic" region $|y| < b/2 - \delta$:

$$\beta E_x = e\nu \ln\left(\frac{b^2/4 - y^2}{(b/2-\delta)^2 - y^2}\right) + 2\int\limits_{\delta-b/2}^{b/2-\delta} \frac{\sigma(y')dy'}{y'-y} \tag{40}$$

where the integral should be understood as the principal value.

Eq. (40) has the following solution (see, e.g., [31]):

$$\sigma(y) = \frac{\pi\beta E_x(b/2-\delta) + e\nu \int\limits_{\delta-b/2}^{b/2-\delta} \ln\left(1+\frac{b\delta-\delta^2}{(b/2-\delta)^2-t^2}\right)\frac{\left[(b/2-\delta)^2-t^2\right]^{1/2}dt}{t-y}}{2\pi^2\left[(b/2-\delta)^2-y^2\right]^{1/2}}. \tag{41}$$

The unknown parameter δ can be found from the condition that Eq. (41) has no singularity at $y = b/2-\delta$. For $\delta \ll b$

this gives

$$\delta = b\left(\frac{\beta E_x}{4e\nu}\right)^2. \tag{42}$$

For any reasonable values of parameters corresponding to the quantum Hall effect, the factor in brackets is much less than unity which justifies our assumption $\delta \ll b$. Knowledge of the charge distribution in the whole sample allows us to calculate by direct integration the electrical potential $\phi(y,0)$ and then the chemical potential $\zeta(y)$ from the relation

$$e\varphi(y,0) - \zeta(y) + \zeta_0 = -\beta E_x y. \tag{43}$$

The exact distribution of electron density, electrical and chemical potential in the sample are shown schematically in Fig. 4a. A similar non-monotonic $\varphi(y,0)$ dependence was earlier obtained by numerical calculations [32, 33].

It is interesting to note that the total charge concentrated in half of the "metallic" region is of order $\beta E_x b$ whereas the charge in the edge "dielectric" strip has a much smaller value $\sim e\nu\delta \sim \beta E_x b(\delta/b)^{1/2}$.

The arguments given above demonstrate that even at low current (small E_x) the electron concentration at opposite Hall edges differ by the finite value: $n(b/2)-n(-b/2) = \nu$. The phenomenon has the same physical reason as a finite potential step of $\hbar\omega_c/e$ for an arbitrary small potential inhomogeneity considered in Sect. 3.2.

Our conclusions are adequate for not very large E_x. If the current (and, hence, E_x) is large enough, the chemical potential ζ varying at the length δ may reach the next LL, causing one more "metallic" strip in the sample. In this case $n(b/2) - n(-b/2)$ becomes equal to 2ν, rather than ν. Let us estimate the corresponding critical value of E_x. It can be shown that $\zeta(b/2)-\zeta_0 \sim e\beta E_x\delta$. An additional strip appears when this difference exceeds $\hbar\omega_c$, which, together with Eq. (42), gives

$$\mu(E_x)_{cr} \sim \left(\frac{e^4}{\hbar m b}\right)^{1/3}. \tag{44}$$

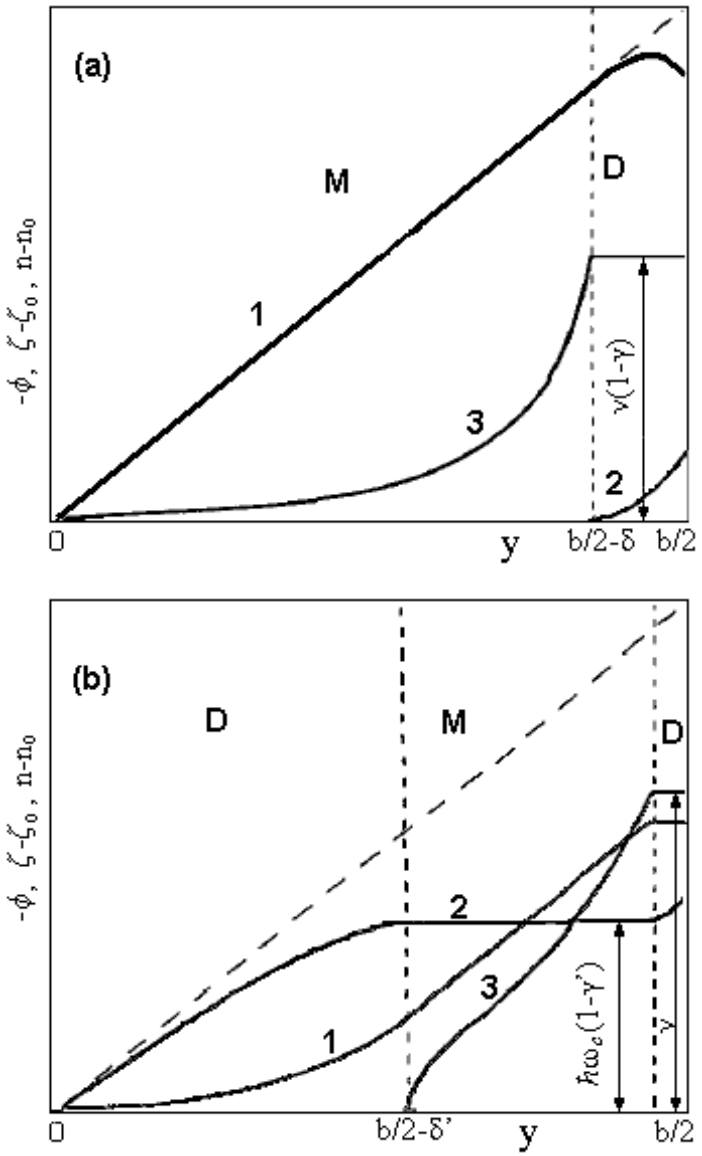

Figure 4: Schematic coordinate dependence of the electrostatic potential (curve 1), chemical potential (curve 2) ana non-compensated electron density (curve 3) under quantum Hall conditions[26]. (a) – non-integer equilibrium filling factor: $n_0 = \nu(N+\gamma)$, $\zeta_0 = \hbar\omega_c(N+1/2)$. (b) – integer filling factor: $n_0 = \nu(N+1)$, $\zeta_0 = \hbar\omega_c(N+1/2+\gamma')$. Letters M and D note "metallic" and "dielectric" regions. Broken lines correspond to the linear dependence $\varphi(y,0) = -\beta E_x y$.

Further increase in E_x will cause the appearance of additional "metallic" strips followed by new jumps in $n(b/2) - n(-b/2)$.

If ζ_0 lies in a gap between LLs, $\zeta_0 = \hbar\omega_c(N + 1/2 + \gamma')$ with $0 < \gamma' < 1$, the situation is rather different. At low currents when eV_H is less than $\hbar\omega_c$, there are no delocalized electrons at the Fermi level. In this case formally $l_2 = \infty$ and screening is provided only by the deformation of Landau wavefunctions [28] which is beyond our approach based on the local connection between the electron density and the

potential. At higher currents the chemical potential level near one or both edges begins to be pinned to a LL, and the local filling factor acquires a non-integer value (qualitatively this factor has already been pointed out [34]). These "metallic" regions provide effective screening and change the potential distribution drastically compared to the low-current case.

To obtain the complete picture of charge and potentials distributions for our case of a "dielectric" sample (Fig. 4b), we assume for illustrative purposes $\gamma' = 1/2$ and find, first of all, the charge distribution $\sigma(y)$ in a "metallic" strip $b/2 - \delta' < y < b/2$. Taking into account that this strip, together with the oppositely charged strip $/b/2 < y < -b/2 + \delta'$, creates inside itself the uniform electric field βE_x (Eq. (38)), we obtain an integral equation for $\sigma(y)$:

$$\beta E_x = -4y \int\limits_{b/2-\delta'}^{b/2} \frac{\sigma(y')dy'}{y'^2 - y^2}. \tag{45}$$

Its solution for $\delta' \ll b/2$ has the form

$$\sigma(y) = -\frac{\beta E_x}{2\pi}\sqrt{\frac{y - b/2 + \delta'}{b/2 - y}}. \tag{46}$$

The expression Eq. (41) diverges at $y = b/2$. This singularity is suppressed by formation of narrow "dielectric" strips with $\sigma = \pm e\nu/2$ near the sample edges. The situation is similar to the earlier considered case $\zeta_0 \simeq \hbar\omega_c(N + 1/2)$ and, as it has been shown, the width and total charge of these strips are very small. Thus everywhere except in the vicinity of the edges we may ignore the existence of these strips and use Eq. (46).

The calculated charge distribution creates the following potential in the

neutral part of the sample $|y| < b/2 - \delta'$:

$$\varphi(y,0) = 2\int\limits_{-b/2}^{b/2} \sigma(y') \ln\left(\frac{y'-y}{y'+y}\right) dy'$$

$$= -\frac{\beta E(b/2-\delta')}{\pi} \int\limits_{0}^{2\delta'} \sqrt{\frac{t}{2\delta'/b-t}} \ln\left(\frac{t+2}{t}\right) dt. \qquad (47)$$

To determine the unknown value δ', we note that, at the point $y = b/2 - \delta'$, ζ must coincide with a LL and hence $\zeta - \zeta_0$ must be equal to $\hbar\omega_c(1-\gamma')$ (or to $-\hbar\omega_c\gamma'$ at the opposite edge). Taking account of Eq. (43), this gives us (for $\gamma' = 0.5$) the equation

$$e\beta E_x \delta' \left[2.4 + \ln(b/\delta')\right] = e\beta E_x b - \hbar\omega_c. \qquad (48)$$

Eq. (48) has solutions compatible with our assumption $\delta' \ll b$ in a rather narrow interval of currents. This means that soon after $e\beta E_x b$ exceeds $\hbar\omega_c$, the "metallic" region covers a considerable part of a sample. As a result, we come to the situation similar to that of non-integer filling factor. The only difference is that $n(b/2) - n(-b/2)$ is equal to 2ν rather than ν.

Therefore, in the conditions of quantum Hall effect there is a large interval of Hall fields, $\hbar\omega_c/eb < \beta E_x < \beta(E_x)_{cr}$, where the electron concentrations at opposite sample edges differ by a constant value ν times integer.

In Sect. 2.2 and in the present section we have shown that even in a completely uniform sample the electron concentration and the Hall electric field are distributed non-uniformly across the sample and in 2D samples this non-uniformity can be large enough. How can these effects be observed experimentally? The question is not so simple. Direct probe measurements cannot help here, since they measure not electrical but electrochemical potential which, contrary to the electrical one, varies linearly with y and is the same as it would be in the absence of effects discussed. What we need, is some experiment, which would measure local values of either electron concentration or electrical (not electrochemical!) field.

First such experiment was performed in [35]. It was based on measurements of the acoustoconductivity of 2D electron gas, that is the change in conductivity under the influence on non-equilibrium phonons. In experiments, the GaAs substrate with the GaAs/AlGaAs heterostructure containing 2D electron gas, was covered from the opposite side by a metallic film locally illuminated by a focused laser beam. The illuminated hot spot is

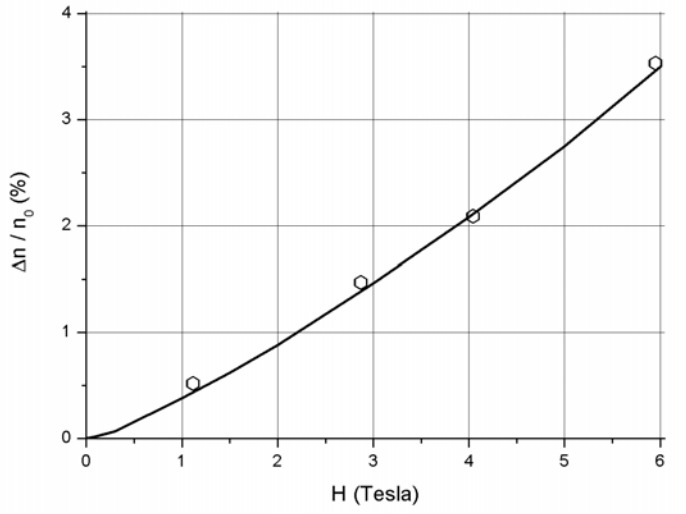

Figure 5: Variation of $n(b/2) - n(-b/2)$ with magnetic field [35]. The effects of internal inhomogeneity have been cancelled by making measurements for both current directions.

a source of non-equilibrium phonons, which, travelling ballistically through the substrate, affect conductivity of the 2D layer in the area just above the hot spot. The experiments were conducted in external high magnetic field perpendicular to the 2D layer. The exact physical mechanism of acoustoconductivity (see, e.g., [35]) is irrelevant for our purposes. What is important, is the fact that acoustoconductivity, as any kinetic coefficient in a high magnetic field, has an oscillating (Shubnikov-de Haas-like) function of magnetic field strength with the period determined by the Fermi energy and, hence, the carrier concentration. In the case of local laser illumination, the determined concentration characterizes the area above the hot spot.

Experiments [35] showed that while scanning the laser beam along the Hall direction, the frequency of such oscillations of the acoustoconductivity amplitude varied monotonically demonstrating the presence of concentration gradient in this direction. This gradient changed the sign with the sign of magnetic field and increased with the field (Fig. 5) confirming that the effect is related not to some internal inhomogeneity of the sample but to the effect of Hall-induced concentration gradient described above.

Another possibility of measuring edge charges in 2D samples, realized in [36], consists in measuring local electro-optical effect giving the value of

electric field in the vicinity of a sample. The authors directly observed noticeable potential drops hear samples edges under conditions of the quantum Hall effect and found that these edge regions penetrate the sample rather deeply (up to hundred micron), in full agreement with weak screening in 2D systems described above.

References

[1] A.Y. Shik, *Electronic Properties of Inhomogeneous Semiconductors* (Gordon and Breach, Amsterdam, 1995).

[2] K. Seeger, *Semiconductor Physics: an Introduction*, 9th ed. (Springer, Berlin, 2004).

[3] D. Stauffer, *Introduction to Percolation Theory* (Taylor and Francis, London, 1985).

[4] B.I. Shklovskii and A.L. Efros, *Electronic Properties of Doped Semiconductors* (Springer, Berlin, 1984).

[5] A.M. Dykhne, Sov. Phys. JETP **32**, 63 (1970).

[6] R. Zallen and H. Scher, Phys. Rev. B **4**, 4471 (1971).

[7] H. Koppe and J.M. Bryan, Canad. J. Phys. **29**, 274 (1951).

[8] A. Shik, JETP Lett. **20**, 5 (1974).

[9] A. Waxman, V.E. Hentich, F.V. Shallcross, H. Borkan, and P.K. Weimer, J. Appl. Phys. **36**, 168 (1965).

[10] J.T.C. Chen and R.S. Muller, J. Appl. Phys. **45**, 828 (1974).

[11] C.A. Ribeiro and J.C. Pfister, Solid State Comm. **10**, 63 (1972).

[12] A.A. Guzev, G.L. Kuryshev, and S.P. Sinitsa, Phys. Stat. Sol. (a) **14**, 41 (1972).

[13] G.F. Neumark, Phys. Rev. B **1**, 2613 (1970).

[14] N. Mott, Electr. and Power **19**, 321 (1973).

[15] D.C. Tsui and S.J. Allen, Phys. Rev. Lett. **34**, 1293 (1975).

[16] N. Mott, M. Pepper, S. Polliot, R.H. Wallis, and C.J. Adkins, Proc. Roy. Soc. London A **345**, 169 (1975).

[17] S.J. Allen, D.C. Tsui, and J.V. Dalton, Phys. Rev. Lett. **32**, 107 (1974).

[18] L.N. Abessonova, V.N. Dobrovol'skii, Yu.S. Zharkikh, G.K. Ninidze, O.S. Frolov, and A.Ya. Shik, Sov. Phys. Semicond. **10**, 244 (1976).

[19] A. Shik, Sov. Phys. Semicond. **9**, 574 (1975).

[20] A. Shik, Sov. Phys. Semicond. **17**, 1422 (1983).

[21] C. Herring, J. Appl. Phys. **31**, 1939 (1960).

[22] S.V. Iordansky, Solid State Comm. **43**, 1 (1982).

[23] R.F. Kazarinov and S. Luryi, Phys. Rev. B **25**, 7626 (1982).

[24] A. Shik, Sov. Phys. Semicond. **9**, 761 (1975).

[25] Yu.A. Dreizin and A.M. Dykhne, Sov. Phys. JETP **36**, 127 (1972).

[26] A. Shik, J. Phys.: Condens. Matt. **5**, 8963 (1993).

[27] A. Shik, Semiconductors **29**, 697 (1995).

[28] A.H. MacDonald, T.M. Rice, and W.F. Brinkman, Phys. Rev. B **28**, 3648 (1983).

[29] D.B. Chklovskii, B.I. Shklovskii, and L.I. Glazman, Phys. Rev. B **46**, 4026 (1992).

[30] S.G. Petrosyan and A.Ya. Shik, Sov. Phys. JETP **69**, 1261 (1989).

[31] F.G. Tricomi, *Integral Equations* (Wiley Interscience, N.Y., 1957).

[32] R.R. Gerhardts and V. Gudmundsson, Solid State Comm. **67**, 845 (1988).

[33] D. Pfannkuche and J. Hajdu, Phys. Rev. B **46**, 7032 (1992).

[34] V.M. Pudalov and S.G. Semenchinskii, JETP Lett. **42**, 232 (1985).

[35] D.J. McKitterick, A. Shik, A.J. Kent, and M. Henini, Phys. Rev. B **49**, 2585 (1994).

[36] W. Dietsche, K. von Klitzing, and K. Ploog, Surf. Sci. **361/362**, 289 (1996).